

Influence of Co substitution on magnetoelastic properties of $\text{Nd}_6\text{Fe}_{13}\text{Cu}$ compound

P. Iranmanesh¹, N. Tajabor^{*1}, M. Rezaee Roknabadi¹, D. Fruchart², F. Pourarian³

1- Department of Physics, Faculty of Sciences, Ferdowsi University of Mashhad, Mashhad, 91775-1436, Iran.

2- Institut Néel, Département MCMF, Group IICF, BP 166, 38042 Grenoble Cedex 9, France

3- Department of Material Science & Engineering, Carnegie Mellon University, Pittsburgh, PA 15219, USA.

(Received: 10/3/2010, in revised form: 21/5/2010)

Abstract: In this research the magnetoelastic properties of $\text{Nd}_6\text{Fe}_{13-x}\text{Co}_x\text{Cu}$ ($x = 0$ and 1) intermetallic compounds are investigated. Analysis of X-ray diffraction patterns indicates that a single phase is formed approximately for $x = 0$ and the $x = 1$ sample is multi-phase. The lattice parameters were decreased, the Néel temperature of main phase and the Curie temperature of impurity phase was increased with Co content. Due to the presence of $\text{Nd}_2\text{Fe}_{17-y}\text{Co}_y$ ferromagnetic phase in the sample with $x = 1$ the change of the anisotropy and increase of exchange effects was observed in the magnetic and magnetoelastic measurements. Thermal expansion, longitudinal (λ_l) and transverse (λ_t) magnetostriction were measured using the strain gauge method in the selected temperatures range of 80 - 500 K under applied magnetic fields up to 1.5 T. Anomaly and Invar effect are observed in the linear thermal expansion and $\alpha(T)$ curves at the Néel temperature. The linear spontaneous magnetostriction decreases sharply by approaching the Néel temperature and also shows the short-range magnetic ordering effects when antiferromagnetic to paramagnetic transition occurs. In the low field region, the absolute values of anisotropic magnetostriction of $\text{Nd}_6\text{Fe}_{13}\text{Cu}$ compound are small and then start to increase with applied magnetic field. Each isofield curve of the anisotropic magnetostriction passes through a minimum and then approaches to zero with increasing temperature. This magnetostriction compensation arises from the difference in the magnetoelastic coupling constants of the sublattices in this compound.

Keywords: Intermetallic compound, $\text{Nd}_6\text{Fe}_{13-x}\text{Co}_x\text{Cu}$, Magnetic properties, Magnetoelastic properties.

Introduction

The ternary intermetallic $\text{RE}_6\text{T}_{13}\text{M}$ compounds (RE = light rare earth, T = Fe or Co, M = Cu, Ag, Au, Si, Ga, etc.) are found as second phase in the M doped RE-Fe-B permanent magnets with enhanced coercivity [1-4]. These compounds crystallize in the tetragonal $\text{Nd}_6\text{Fe}_{13}\text{Si}$ or $\text{La}_6\text{Co}_{11}\text{Ga}_3$ structure with the $I4/mcm$ space group. In this structure, the rare earth ions and M atom occupy $R_1(8f)$, $R_2(16l)$ and $(4a)$ sites and Fe atoms located on the $\text{Fe}_1(4d)$, $\text{Fe}_2(16k)$, $\text{Fe}_3(16l_1)$ and $\text{Fe}_4(16l_2)$ nonequivalent crystallographic sites [2-7]. In addition, they absorb a large amount of hydrogen without any change in their symmetry [5,

6]. Hence, they may provoke some interests in technological field and fundamental investigations. A complicated crystallographic structure and different competing interactions has induced great debates about their spin configuration and magnetic behaviour [8-12].

$\text{Nd}_6\text{Fe}_{13}\text{Cu}$ compound with an antiferromagnetic structure and Néel temperature (T_N) of 419 K was reported before [10] but to our knowledge the substitution of Co for Fe has not been studied yet. The partial replacement of transition elements for Fe usually affects the effective interactions such as crystalline field and magnetic exchanges. Therefore, interesting

*Corresponding author, Telefax: +98 (0511) 8763647, Email: ntajabor@yahoo.com

phenomena are expected in the magnetic and the magnetoelastic properties, though just a few attentions have been paid to the former until now.

Experimental

$\text{Nd}_6\text{Fe}_{13-x}\text{Co}_x\text{Cu}$ ($x = 0$ and 1) compounds were prepared by arc melting of the pure elements (99.9%) under purified Ar atmosphere. The samples were remelted in a high-frequency induction furnace equipped with a water-cooled crucible. To assure the homogeneity, the ingots were subsequently wrapped in a Ta foil, sealed in an evacuated quartz lump, and annealed for 40 days at 550°C [5].

The crystal structure of the samples was determined by X-ray diffraction using $\text{Cu-K}\alpha$ radiation. The analysis of XRD patterns were carried out using Fullprof software and the weight percentage of each phase in the samples was deduced from the intensities of the Bragg's peaks. To determine the Curie temperature of samples, the accurate thermomagnetic measurements were performed on encapsulated free powder with heating rate of $5^\circ\text{C}/\text{min}$ at a constant magnetic field of 0.3 T . The accuracy of the temperature and magnetisation measurements was 0.1 K and 1×10^{-3} a.u. (Arbitrary unit), respectively. The magnetisation measurements of compacted powder were performed at the applied magnetic fields up to 7 T by using a commercial extracting sample magnetometer (ESM) in the temperature ranging from 5 to 300 K .

Linear thermal expansion (LTE) and magnetostriction measurements were performed on

a disc shape sample with 6 mm diameter and 2 mm thickness, in a temperature ranging from 80 to 500 K in magnetic fields up to 1.5 T , using the strain gauge method. No difference was observed between the strains measured in the plane or perpendicular to the plane (cooling direction after the melt) of the disc of the annealed samples, suggesting the absence of any preferred orientation effects. The thermal expansion $\Delta l/l = [l(T) - l(80\text{K})]/l(80\text{K})$ was deduced by measuring the relative change of length of the samples versus temperature. The magnetostriction coefficients were measured (with the accuracy of 2×10^{-6}) parallel (longitudinal magnetostriction, λ_l) and perpendicular (transverse magnetostriction, λ_t) to the field direction, thus allowing to deduce the anisotropic ($\Delta\lambda = \lambda_l - \lambda_t$) magnetostriction.

Results and Discussion

Structural analysis

Analysis of the XRD patterns of $\text{Nd}_6\text{Fe}_{13-x}\text{Co}_x\text{Cu}$ ($x = 0$ and 1) samples shows that for $x = 0$ an approximately single phase $\text{Nd}_6\text{Fe}_{13}\text{Cu}$ compound (containing $\leq 5\text{ wt\%}$ $\text{Nd}_2\text{Fe}_{17}$ phase) with the expected tetragonal structure (S.G. $I4/mcm$) is formed. Upon Co substitution, the second phase $\text{Nd}_2\text{Fe}_{17-y}\text{Co}_y$ with $0 < y < 1$ is formed in the sample (Fig. 1). The data of the X-ray analysis are given in Table 1, which show that the substitution of Co for Fe causes the decrease of the lattice parameters in each individual phase. This is expected because of the smaller size of the cobalt ions with respect to that of iron.

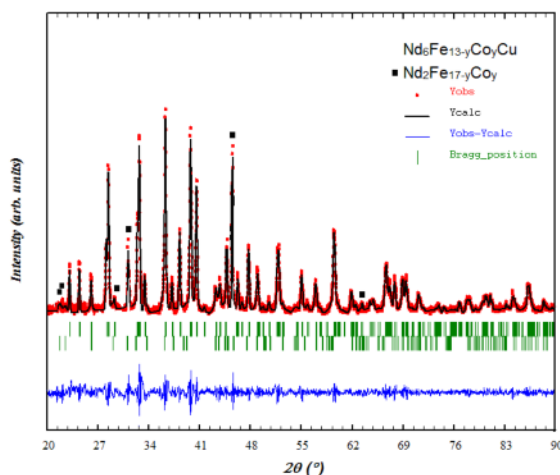


Fig. 1 The observed (circles) and calculated (solid lines) X-ray diffraction patterns of the $\text{Nd}_6\text{Fe}_{12}\text{CoCu}$ sample at room temperature. The vertical bars indicate the position of Bragg reflections and the difference between the observed and calculated intensities is given at the bottom of the diagram. The first and second rows of vertical lines refer to the $\text{Nd}_6\text{Fe}_{12}\text{CoCu}$ and $\text{Nd}_2\text{Fe}_{17-y}\text{Co}_y$ contributions to diffraction pattern.

Table 1. The lattice parameters and unit-cell volumes of $\text{Nd}_6\text{Fe}_{13-x}\text{Co}_x\text{Cu}$ ($x = 0$ and 1) samples.

Sample	Compound	wt%	a (Å)	c (Å)	V (Å ³)
x = 0	$\text{Nd}_6\text{Fe}_{13}\text{Cu}$	≈ 95	8.0962	22.2791	1460.360
	$\text{Nd}_2\text{Fe}_{17}$	≤ 5	8.5782	12.4611	794.108
x = 1	$\text{Nd}_6\text{Fe}_{13-y}\text{Co}_y\text{Cu}$	74	8.0957	22.2757	1459.963
	$\text{Nd}_2\text{Fe}_{17-y}\text{Co}_y$	26	8.5748	12.4573	793.234

Magnetic properties

The Curie temperature of the prepared samples with $x = 0$ and 1 which obtained from the second derivative of magnetisation versus temperature curves, are 325 and 403, respectively. It is believed that these observed Curie temperatures are due to the presence of the impurity phases of $\text{Nd}_2\text{Fe}_{17}$ and $\text{Nd}_2\text{Fe}_{17-y}\text{Co}_y$ ($0 < y < 1$) in the samples [13].

The temperature dependence of the magnetisation for $x = 0$ and 1 samples at selected

fields are shown in Fig. 2. It can be seen that the magnetisation curves for $x = 0$ sample show a hill shape region in a temperature range depending on the strength of the magnetic field. The anomalously rise in magnetisation in the range from 30 to 150 K may attribute to a canting configuration of the moments of sublattices that causes enhancement of the resultant magnetisation. This behaviour is also reported for $\text{Pr}_6\text{Fe}_{13}\text{Sn}$ compound [3].

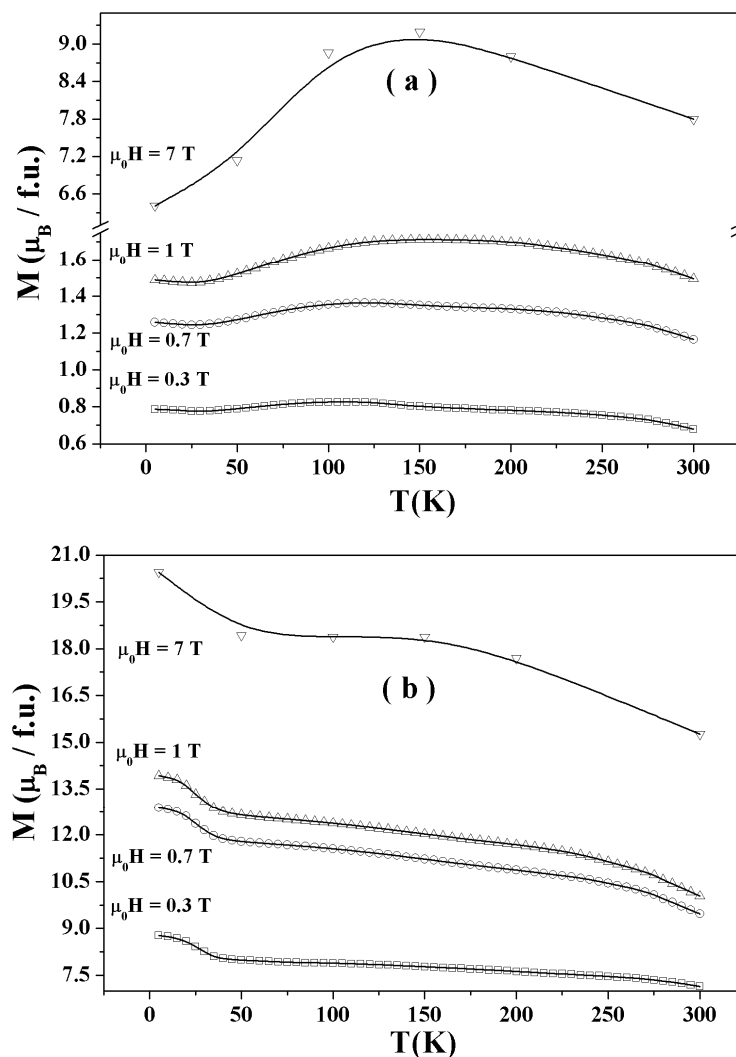


Fig. 2 Temperature dependence of the magnetisation of $\text{Nd}_6\text{Fe}_{13-x}\text{Co}_x\text{Cu}$ (a) $x = 0$ and (b) $x = 1$ samples at different applied fields.

A low value of magnetisation ($M < 8 \mu_B/\text{f.u.}$) at 300 K and 7 T for the sample with $x = 0$ confirms that the magnetic structure consists of at least two magnetic sublattices which are aligned antiparallel as depicted in Fig. 3. In the $\text{RE}_6\text{T}_{13}\text{M}$ family of compounds, the short-range magnetic orders may originate from the Fe-Fe exchange interactions. These magnetic correlations usually are considered as primary step for expanding a macroscopically ordered magnetic phase over the volume of magnetic materials [16]. Considering structure of the studied compound in Fig. 3, the preliminary short-range magnetic orders can be originated from n_{FeFe} intralayer ferromagnetic exchange interaction. However, the long-range order starts by activation of the Fe ($16l_2$)-Nd ($8f$) interlayer planar ferromagnetic interaction (n_{RFe}), and will be completed by the antiferromagnetic arrangement of the blocks separated by the nonmagnetic M slabs. However, we know that the magnetisation curve of the sample with $x = 1$ represents the total magnetisation of $\text{Nd}_6\text{Fe}_{13-y}\text{Co}_y\text{Cu}$ and $\text{Nd}_2\text{Fe}_{17-y}\text{Co}_y$ phases. At low fields, the sample behaves as a ferromagnetic system due to the magnetisation of the $\text{Nd}_2\text{Fe}_{17}$ -based compound, and then as the magnetic field increases the magnetisation of $\text{Nd}_6\text{Fe}_{13}\text{Cu}$ -based compound also contributes to the total magnetisation.

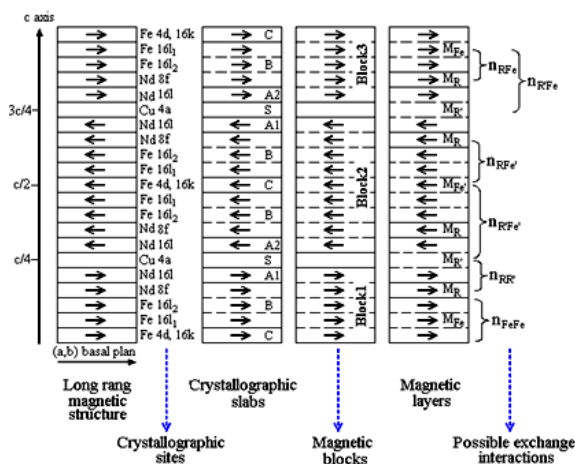


Fig. 3 The conventional concepts in description of the crystal and magnetic structure of Nd₆Fe₁₃Cu compound based on the Mössbauer spectral studies [14, 15]. Estimation of the exchange field parameters shows that $|n_{\text{RFe}}|$ ($|n_{\text{RFe}}|_{-}$) $< |n_{\text{RR}}| < |n_{\text{FeFe}}| \ll |n_{\text{RFe}}| < |n_{\text{FeFe}}|$, and n_{RFe} .

1- Bohr magneton per formula unit

Magnetoelastic properties

Fig. 4 shows linear thermal expansion, $\Delta l/l(T)$, of samples with $x = 0$ and 1, as well as the LTE coefficient, $\alpha(T) = d/dT[\Delta l/l(T)]$, deduced from the slope of the experimental curve of the linear thermal expansion at selected temperatures. The Néel temperatures are indicated by the arrows. It can be seen that, both $\Delta l/l(T)$ and $\alpha(T)$ curves show anomaly and Invar effect by approaching T_N . The linear thermal expansion coefficient curve beyond the magnetic ordering temperature in the paramagnetic region is almost linear. The observed Néel temperature of $\text{Nd}_6\text{Fe}_{13}\text{Cu}$ is approximately 421 K that is in agreement to the reported value [10]. In Fig. 4(b) for sample with $x = 1$, there are two anomalies in the linear thermal expansion coefficient curve, the first minimum is about 403 K and the second one is about 452 K. We believe that the first anomaly belongs to the Curie temperature of $\text{Nd}_2\text{Fe}_{17-y}\text{Co}_y$ and the second one may refers to the Néel temperature of the $\text{Nd}_6\text{Fe}_{13-y}\text{Co}_y\text{Cu}$ compound.

Below the magnetic ordering temperature, the measured linear thermal expansion $(\Delta l/l(T))_{exp}$ of the magnetic materials is the combination of lattice $(\Delta l/l(T))_{latt}$ and magnetic $(\Delta l/l(T))_m$ contributions. In order to calculate the lattice contribution, the measured thermal expansion in the paramagnetic region has been fitted using Grüneisen–Debye model with Debye temperature $T_D = 314$ K [15]. Therefore, the magnetic contribution or the so called linear spontaneous magnetostriction is the difference between experimental and the lattice thermal expansion $(\Delta l/l(T))_m = (\Delta l/l(T))_{exp} - (\Delta l/l(T))_{latt}$; which refers to the change of magnetic energy due to the temperature dependence of the crystallographic unit cell volume. The obtained linear spontaneous magnetostriction for samples with $x = 0$ and 1 is presented in Fig. 5. Considering the schematic representation of collinear antiferromagnetic structure of $Nd_6Fe_{13}Cu$ compound in Fig. 3, the linear spontaneous magnetostriction of this compound below $T_N = 421$ K can be attributed to the gradual occurrence of the long-range ordering of the magnetic moments. The small value of linear spontaneous magnetostriction beyond the magnetic ordering temperature may arise from the short-range magnetic ordering that has been observed in several R-T intermetallic compounds [17].

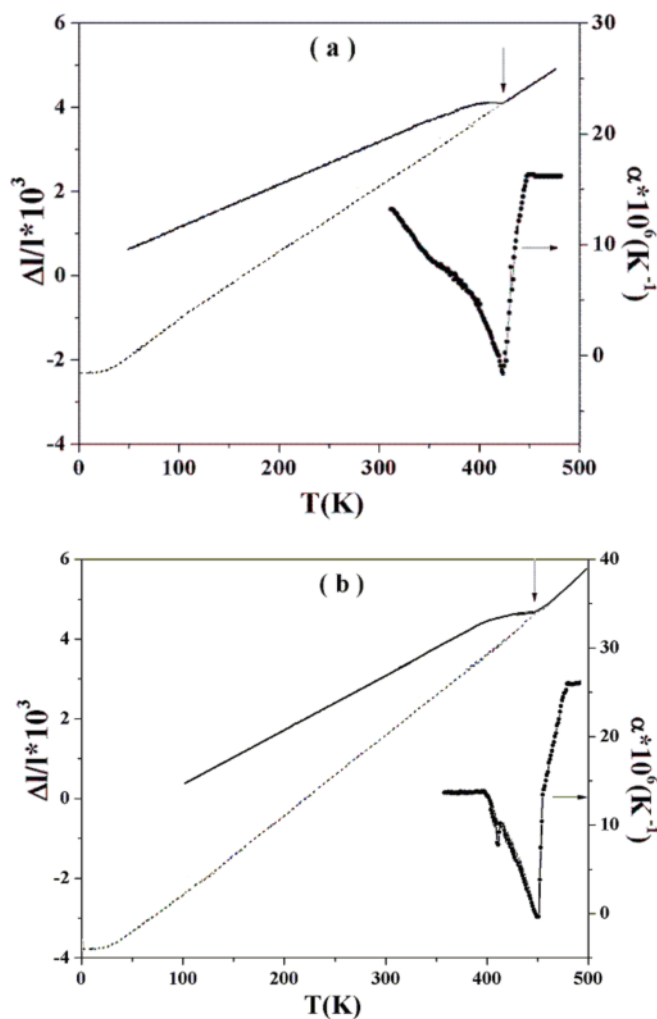


Fig. 4 Experimental thermal expansion $\Delta l/l(T)$ and linear thermal expansion coefficient $\alpha(T)$ curve of $\text{Nd}_6\text{Fe}_{13-x}\text{Co}_x\text{Cu}$ (a) $x = 0$ and (b) $x = 1$ samples. The dash line exhibits calculated lattice contribution to the thermal expansion. The arrows indicate the Néel temperature.

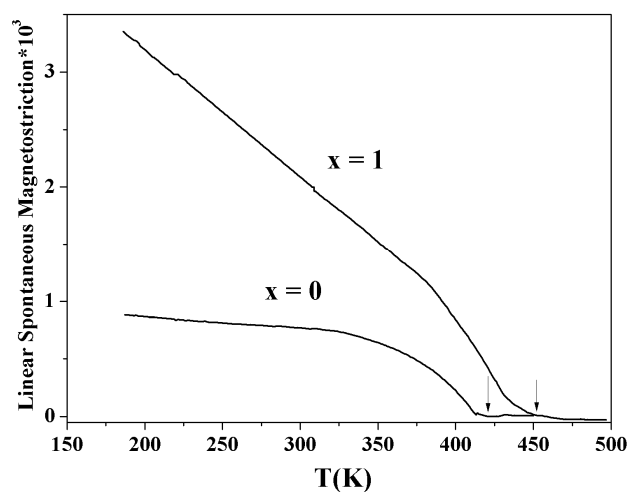


Fig. 5 Temperature dependence of the linear spontaneous magnetostriction of $\text{Nd}_6\text{Fe}_{13-x}\text{Co}_x\text{Cu}$ (a) $x = 0$ and (b) $x = 1$ samples. Arrows indicate the beginning of the paramagnetic behaviour.

The anisotropic magnetostriction ($\Delta\lambda$) curves as a function of applied magnetic field are shown in Fig. 6. It can be seen that at first in Fig. 6(a), the absolute value of $\Delta\lambda$ in the $\text{Nd}_6\text{Fe}_{13}\text{Cu}$ compound is small and then increases with applied field at temperatures below 145 K. Saturation behaviour starts approximately from 200 K. This trend may be attributed to the temperature dependence of the magnetostriction constants behaviour.

The temperature dependence of the anisotropic magnetostriction at selected fields is also represented in Fig 7. All the curves of $\text{Nd}_6\text{Fe}_{13}\text{Cu}$ compound in Fig. 7(a) have similar behaviour in whole temperature range; the absolute value of $\Delta\lambda$ first increases with temperature up to about 145 K and then decreases to zero at magnetostriction compensation point that occurs above the room temperature.

Pervious results on the $\text{R}_6\text{Fe}_{13}\text{M}$ compounds

show the existence of two rare earth sites with the opposite anisotropy. This means that these two sites have different easy directions (the 16l and 8f sites exhibit uniaxial and nearly planar anisotropy, respectively) [5, 18]. So, the magnetostrictive strain with different sign can be expected at these two Nd sites. It is also found that the compensation point and spin reorientation transition in $\text{Nd}_6\text{Fe}_{13}\text{Si}$ compound coincide together [19]. Below T_{SR} , the overall spin arrangement of the Nd(8f) and Fe atoms is planar. From these experimental facts we can deduce the magnetostrictive strain sign of the two Nd sites and the Fe sublattice. The value of $\Delta\lambda$ in $\text{Nd}_6\text{Fe}_{13}\text{Si}$ below T_{SR} is negative. Since the anisotropy of the rare earth sublattice dominants at low temperatures, therefore the Nd(8f) site with planar anisotropy creates negative strain. Above T_{SR} and at high temperatures, the Nd(16l) site and Fe sublattice with axial anisotropy have positive contribution to the $\Delta\lambda$ results.

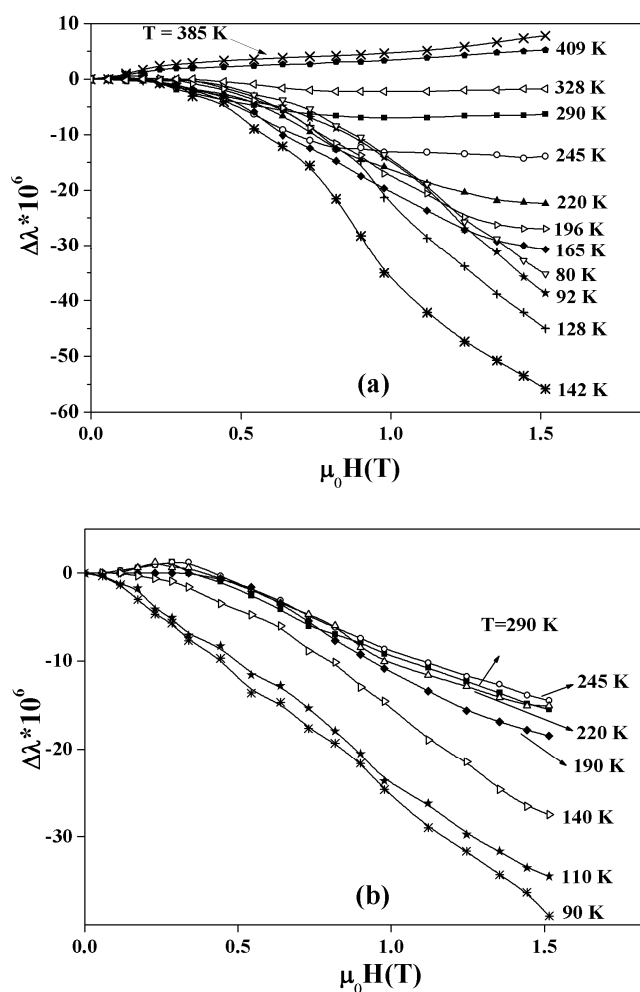


Fig. 6 Isothermal curves of the anisotropic magnetostriction of $\text{Nd}_6\text{Fe}_{13-x}\text{Co}_x\text{Cu}$ (a) $x = 0$ and (b) $x = 1$ samples as a function of applied field at selected temperatures.

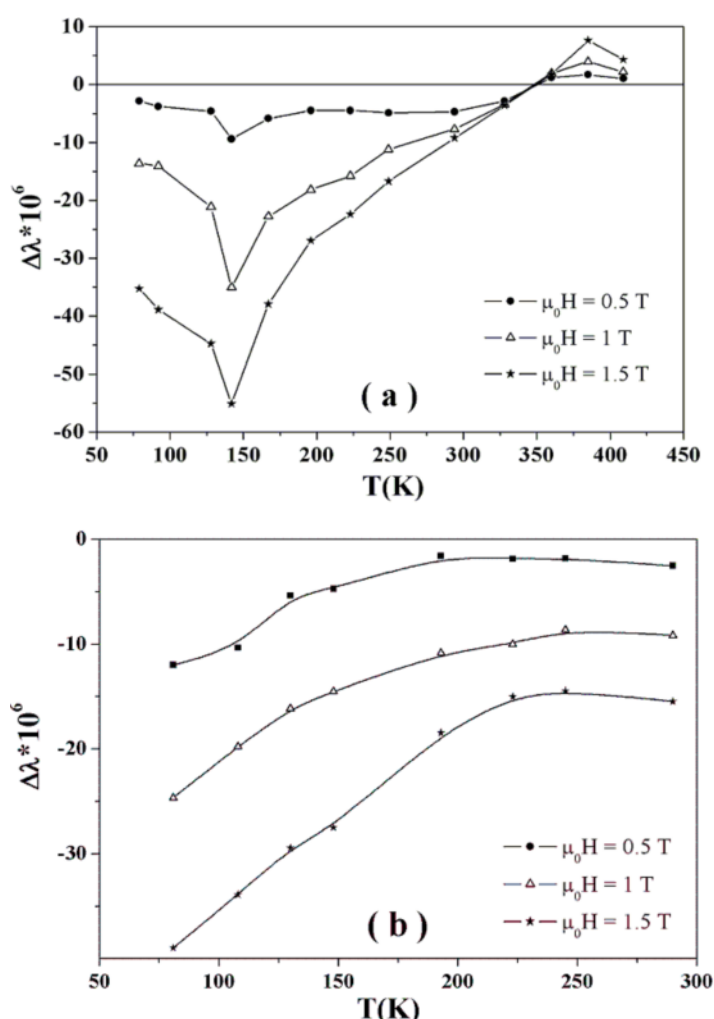


Fig. 7 Temperature dependence of the anisotropic magnetostriction $\text{Nd}_6\text{Fe}_{13-x}\text{Co}_x\text{Cu}$ (a) $x = 0$ and (b) $x = 1$ samples at selected applied fields.

By comparing the anisotropic magnetostriction results of $\text{Nd}_6\text{Fe}_{13}\text{Si}$ with that of the $\text{Nd}_6\text{Fe}_{13}\text{Cu}$ compound in Fig. 7(a), it can be concluded that by increasing the temperature the negative contribution of Nd (8f) site to $\Delta\lambda$ increases up to about 145 K, where $\Delta\lambda$ curves approach minimum. Then, as the temperature increases, the positive contribution of the Fe sublattice in magnetostriction compete more with negative contribution of Nd (8f) site. Finally, these two contributions compensate each other and the anisotropic magnetostriction goes to zero ($T_0 \approx 350$ K). Similar magnetostriction compensation behaviour has also been reported for $\text{Pr}_6\text{Fe}_{11}\text{Ga}_3$ [16]. After passing the compensation point, the positive value of Fe planar sublattice to $\Delta\lambda$ increases and dominates that of the Nd(8f) site. By approaching ordering temperature, $\Delta\lambda$ becomes zero.

$\Delta\lambda$ in Fig. 7(b) for sample with $x = 1$ follows the same trend as magnetisation curves in Fig. 2(b). Due to the presence of large amount of the second phase of $\text{Nd}_2\text{Fe}_{17-y}\text{Co}_y$ in the studied sample it is difficult to precisely analyze the above data.

Conclusion

Linear thermal expansion and magnetostriction behaviour of $\text{Nd}_6\text{Fe}_{13-x}\text{Co}_x\text{Cu}$ ($x = 0$ and 1) compounds are studied. From the analysis of XRD patterns and thermomagnetic results it can be concluded that by Co substitution, the lattice parameters of each individual phase are decreased with increase in T_C and T_N . The magnetisation curve of the sample with $x = 0$ ($\text{Nd}_6\text{Fe}_{13}\text{Cu}$ compound) shows a hill shape region and this may be attributed to the canting configuration of the magnetic moments of the sublattices. This canting configuration originates from the competition between the magnetic anisotropy and the thermal

energy that changes canting angle between the magnetic moments and the applied magnetic field. The magnetic behaviour of the sample with $x = 1$ at low fields may be dominated by the presence of the $\text{Nd}_2\text{Fe}_{17-y}\text{Co}_y$ phase. Well defined anomalies and Invar effect are observed in the linear thermal expansion and $\alpha(T)$ curves at the Néel temperature. The linear spontaneous magnetostriction decreases sharply by approaching the Néel temperature and also shows the short-range magnetic ordering effects when antiferromagnetic to paramagnetic transition occurs. In the sample with $x = 1$, there are two anomalies in the α curve, the first one is about 403 K which belongs to the Curie temperature of $\text{Nd}_2\text{Fe}_{17-y}\text{Co}_y$ compound and the second minimum is about 452 K which may refers to the Néel temperature of the $\text{Nd}_6\text{Fe}_{13-y}\text{Co}_y\text{Cu}$ compound.

In the sample with $x = 0$, temperature dependence curves of anisotropic magnetostriction pass through a minimum at about 145 K and then go to zero at compensation temperature ($T_0 \approx 350$ K). This behaviour shows that the anisotropy of the Nd and Fe sublattices with different sing compete with each other. In the sample with $x = 1$, due to the presence of large amount of the second phase of $\text{Nd}_2\text{Fe}_{17-y}\text{Co}_y$ in the studied sample it is difficult to precisely analyze the anisotropic magnetostriction behaviour.

Acknowledgement

The authors would like to thank the financial support from the Faculty of Sciences, Ferdowsi University of Mashhad under Grant No.1242/p date 10.11.2007.

References

- [1] Weitzer F., Leithe-Jasper A., Rogl P., Hiebl K., Rainbacher A., Wiesinger G., Steiner W., J. Fried, Wagner F. E., "J. Appl. Phys.", 75 (1994) 7745-7751.
- [2] Leithe-Jasper A., Rogl P., Wiesinger G., Rainbacher A., Hatzl R., Forsthuber M., "J. Magn. Magn. Mater.", 170 (1997) 189-200.
- [3] Xiao Q.F., Zhao T., Zhang Z.D., Yu M.H., Zhao X.G., Liu W., Geng D.Y., Sun X.K., de Boer F.R., "J. Magn. Magn. Mater.", 184 (1998) 330-336.
- [4] Isnard O., Long G.J., Hautot D., Buschow K.H.J., Grandjean F., "J. Phys. Condens. Matter", 14 (2002) 12391-12409.
- [5] Knoch K.G., Le Calvez A., Qi Q., Leithe-Jasper A., Coey J.M.D., "J. Appl. Phys.", 73 (1993) 5878-5880.
- [6] Coey J.M.D., Qi Q., Knoch K.G., Leithe-Jasper A., Rogl P., "J. Magn. Magn. Mater.", 129 (1994) 87-97.
- [7] Wang F., Wang J., Zhang P., Shen B.G., Yan Q., Zhang L., "Physica B", 269 (1999) 17-21.
- [8] Schobinger-Papamantellos P., Buschow K.H.J., de Groot C.H., de Boer F.R., Ritter C., Fauth F., Boettger G., "J. Alloys Comp.", 280 (1998) 44-55.
- [9] Kennedy S.J., Wu E., Wang F.W., Zhang P.L., Yan Q.W., "Physica B", 276-278 (2000) 622-623.
- [10] de Groot C.H., Buschow K.H.J., de Boer F.R., "Phys. Rev. B", 57 (1998) 11472-11482.
- [11] Schobinger-Papamantellos P., Buschow K.H.J., Ritter C., "J. Alloys and Comp.", 359 (2003) 10-12.
- [12] Grandjean F., Long G.J., Guillo M., Isnard O., Buschow K.H.J., "Phys. Condens. Matter", 16 (2004) 4347-4355.
- [13] Radhakrishna Umarji P., Murthy A.M., Narasimha V.G., "Modern Physics Letters B", 6 (1992) 1449-1453.
- [14] Hautot D., Long G.J., Grandjean F., de Groot C.H., Buschow K.H.J., "J. Appl. Phys.", 81 (1997) 5435-5437.
- [15] Hautot D., Long G.J., Grandjean F., de Groot C.H., Buschow K.H.J., "J. Appl. Phys.", 83 (1998) 1554-1562.
- [16] Alinejad M.R., Tajabor N., Pourarian F., "J. Magn. Magn. Mater.", 320 (2008) 2140-2143.
- [17] Wang J.L., Ibarra M.R., Marquina C., García-Landa B., Tegus O., Xiao Q.F., Brück E., Yang F.M., Wu G.H., "J. Appl. Phys.", 91 (2002) 8216-8218.
- [18] Li H.S., Hu B.P., Cadogan J.M., Gavigan J.P., "J. Appl. Phys.", 67 (1990) 4841-4843.
- [19] Tajabor N., Alinejad M.R., Pourarian F., "Physica B", 321 (2002) 60-62.